Available online at www.sciencedirect.com
ScienceDirect
C. R. Mecanique 337 (2009) 352–361
COMPTES RENDUS MECANIQUE

Combustion for aerospace propulsion

Comparison of numerical methods and combustion models for LES of a ramjet

A. Roux [a,*], S. Reichstadt [b], N. Bertier [b], L. Gicquel [a], F. Vuillot [b], T. Poinsot [c]

[a] *CERFACS, 52, avenue G. Coriolis, 31057 Toulouse cedex, France*
[b] *ONERA, BP 72, 29, avenue de la Division Leclerc, 92322 Châtillon cedex, France*
[c] *IMFT, avenue C. Soula, 31400 Toulouse, France*

Available online 21 July 2009

Abstract

Ramjets are very sensitive to instabilities and their numerical predictions can only be addressed adequately by Large Eddy Simulation (LES). With this technique, solvers can be implicit or explicit and handle structured, unstructured or hybrid meshes, etc. Turbulence and combustion models are other sources of differences. The impact of these options is here investigated for the ONERA ramjet burner. To do so, two LES codes developed by ONERA and CERFACS compute one stable operating condition. Preliminary LES results of the two codes underline the overall robustness of LES. Mean flow features at the various critical sections are reasonably well predicted by both codes. Disagreement mainly appear in the chamber where combustion positions differ pointing to the importance of the combustion and subgrid mixing models. The two LES produce different energy containing motions. With CEDRE, a low frequency dominates while AVBP produces different ranges of low frequencies that can be linked with acoustic modes of the configuration. ***To cite this article: A. Roux et al., C. R. Mecanique 337 (2009).***

Résumé

Stratégie numérique pour la simulation aux grandes échelles de statoréacteurs. L'impact des méthodes numériques ainsi que du modèle de combustion sur la simulation aux grandes échelles d'un statofusée étudié expérimentalement par l'ONERA est analysé. Pour ce faire, deux codes développés respectivement par l'ONERA et le CERFACS sont utilisés pour calculer un point de fonctionnement stable. Les caractéristiques moyennes sont raisonnablement bien prédites par les deux codes. Les désaccords apparaissent dans la chambre de combustion où la position des zones réactives diffèrent soulignant l'importance des modèles utilisés. Les deux SGE produisent des contenus énergétiques fréquentiels différents. Avec CEDRE, une basse fréquence domine le spectre tandis qu'AVBP montre toute une gamme de basses fréquences qui peut être liée aux modes acoustiques de la configuration. ***Pour citer cet article : A. Roux et al., C. R. Mecanique 337 (2009).***

Keywords: Computational fluid mechanics; Ramjet; Acoustic; Combustion; Numerical methods

Mots-clés : Mécanique des fluides numérique ; Statofusée ; Acoustique ; Combustion ; Méthodes numériques

* Corresponding author.
E-mail address: anthony.roux@cerfacs.fr (A. Roux).

1631-0721/$ – see front matter
doi:10.1016/j.crme.2009.06.008

1. Introduction

Recent numerical progresses in Large Eddy Simulation (LES) [1–3] and development of powerful parallel computers (www.top500.org) have allowed simulations of more and more complex geometries, such as gas turbines [4]. The different phenomenon appearing in these configurations, such as thermo-acoustic coupling or ignition, are well-addressed with the unsteady form of LES. LES of ramjet has, however, received less attention, although in the early 1990s, massive effort coming from the military allowed new designs for such devices. If these configurations are simple in their geometry when no flame holder is used, physical complex phenomena make them hard to simulate: flame stabilization is very complex and strongly influenced by flow structures, wall heat fluxes are high because the flame develops in the vicinity of shear layers near combustor's structure. Two main type of instabilities [5–7] can appear in such combustors and are essentially due to interactions between combustion, acoustic and turbulence that can lead to non-desired operating conditions of the chamber or its destruction. The first type of instability appears at low frequency and is linked with pressure oscillations in the whole device which can deteriorate air breathing and imperfect combustion. The second instability, at higher frequencies and called "screech", is linked with transverse acoustic activity. Surprisingly, this kind of oscillation appears for good and stable combustion, but can lead to the destruction of wall thermal protections.

In 1995, the French National Aerospace Lab ONERA has launched a program named "Research ramjet" to explore the physical phenomena present in such a kind of geometry. It also aims at validating numerical codes thanks to extended experimental data. Two experiments are conducted: a first one aims at describing mixing inside the main chamber as well as the main flow structures for the non-reacting flow of the experimental ramjet. This experiment is of primary interest because of the strong variation of the equivalent ratio in the "dome zone", the downstream zone of the main chamber placed before the air inlet. It has been shown that predicting mixing was hardly possible with Reynolds Average Numerical Simulation (RANS) whereas Large Eddy Simulation method (LES) gives good agreement with the experiment [8–10]. A second experiment explores reacting flows inside a dump combustor with two opposed lateral air inlet curved at 45°.

This article describes the use of two LES codes with different numerical methods to treat convection, time integration and different combustion models. It is shown that even if the codes are very different, they both show good agreement with the experimental data, underlying the robustness and maturity of this advanced numerical approach.

2. Numerical tools for Large Eddy Simulation

The two codes are designed to simulate reactive flows in industrial devices. Nevertheless, they differ in their scope of application. AVBP is an academic LES tool with the main focus on aeronautic or automobile combustion chambers and is largely distributed. CEDRE is a research and industrial tool with its main focus on the general field of energetics and propulsion, covering the full spectrum of aeronautic and aerospace applications (including conception activities for several industrial partners). Its distribution is controlled. They both solve the complete multi-component reactive compressible Navier–Stokes system under conservative formulation, with a finite volume approach on unstructured meshes. They were designed to run on parallel computers and exhibit good scalability properties. Except for the turbulent and combustion modeling, detailed thereafter, the two codes share similar models: perfect gas equation of state, real gas capabilities, heat capacities depending on temperature, heat and diffusion fluxes closed by a basic gradient formulation. However, historically, the difference between the two codes lead to complementary characteristics:

- AVBP was conceived directly for LES and the emphasis was put on the accuracy of numerical schemes which is of third order in space and time thanks to the TTGC scheme for convective flux. Moreover, the fact that this scheme is centered allows it to remain accurate for high wave-numbers (i.e. short wavelengths). The temporal integration is carried out using an explicit scheme. The mesh is unstructured, composed of tetrahedrons, or hybrid (tetrahedrons and prisms), and degrees of freedom are located at the cell's nodes (cell-vertex formulation).
- CEDRE was first intended for RANS approaches, then for LES. Being able to have the same code for both approaches rationalizes developments (sharing of code architecture and IHM) and allows one to initialize the calculations easily with a RANS solution and above all, to move towards hybrid approaches such as Delayed Detached Eddy Simulation (DDES). The code accepts generalized unstructured meshes (made of general polyhedra) including structured, hybrid and imbedded Cartesian grids. Degrees of freedom are located at the center of cells

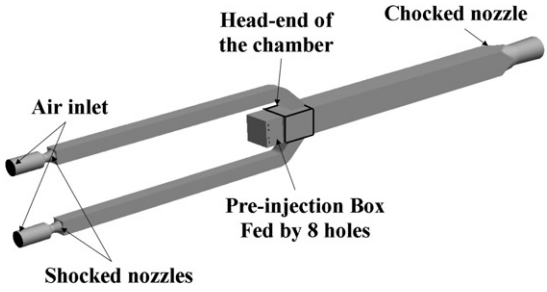

Fig. 1. Computational domain and boundary conditions.

(cell centered). The numerical method is based on a MUSCL (Monotonic Upstream Scheme for Conservations Laws) approach, with Roe-type upwind fluxes. The method is usually second order accurate (third order on uniform mesh) and upwind schemes can easily take into account discontinuities, such as shocks, which allows the code to be used on a wide range of Mach numbers from almost incompressible (using low Mach preconditioning) up to hypersonic. Time integration can be explicit or implicit and proposes an adaptive local time stepping. These numerical properties can be used to run the code in a very robust setting which ease the convergence of complex cases. The implicit time integration allows a large flexibility in the choice of time steps which is virtually not limited by stability conditions while requiring vigilance to stay accurate on most of representative phenomena. However, when used, implicit approaches significantly reduce the cost of computation.

3. Description of the experimental facility

The dump combustor is depicted on Fig. 1. It is composed of two air inlets beginning with a shocked nozzle. They open into the main combustion chamber with a 100×100 mm^2 rectangular cross-section area. Burning fuel, gaseous propane, is injected in the head end through the intermediary of a pre-injection chamber by two 11 mm diameter fuel circular inlets. The combustion chamber is 1261 mm long and opens into a chocked nozzle which has a minimum circular cross-section area with a diameter of 55.8 mm.

This configuration has been accurately studied by ONERA [9,11–13]. Particle Doppler Anemometer (PDA), Laser Doppler Velocimetry (LDV) and Particle Imagery Velocity (PIV) measurements provide experimental data for mean and oscillating velocities. Combustion is quantified thanks to Particle Laser Induced Fluorescence (PLIF) based on OH or CH emission. A high speed camera (up to a resolution of 2000 Hz) gives a view of the flame and microphones characterize pressure oscillations within the ramjet.

Several flight conditions have been experimentally evaluated: inlet temperature and mass flow rate change from 520 K, 2.9 kg s^{-1} to 750 K, 0.9 kg s^{-1}. A range of equivalent ratios, ϕ (from 0.35 to 1.0), has been investigated. The following work focuses on a high altitude regime with a mass flow rate of 0.9 kg s^{-1} and an inlet total temperature of 750 K for a global equivalent ratio of 0.75. The associated Reynolds number, based on the inlet duct, is $\mathrm{Re} = 3.3 \times 10^5$.

4. Numerical parameters

4.1. Computational domain and boundary conditions

The boundary conditions used in the LES are summarized in Table 1. Inclusion of nozzle at both inlets and outlet leads to proper definition of acoustic motions inside the ramjet. Walls are adiabatic. This last point can be discussed since water cooling is applied during the experiment as flames develop in the vicinity of the walls. However, it is not the aim of this study. As strong velocities are found in the three nozzles, they are taken as slip walls to avoid steep gradients.

The mesh used by CEDRE is composed of 3,400,000 hexahedra (around 3,500,000 points) and the AVBP one gathers around 4,500,000 tetrahedra (around 910,000 points). In the head-end of the combustor, the average edge's size is of 1.6 mm for AVBP and 1 mm for CEDRE.

Table 1
Boundary conditions in the LES simulations.

Name	CEDRE	AVBP	Imposed quantities
Air inlet	Subsonic inlet	Non-reflecting inlet	$\dot{Q}_{\text{air}} = 0.9\ \text{kg s}^{-1}$, $T_i = 750\ \text{K}$
Fuel inlet	Subsonic inlet	Non-reflecting inlet	$\dot{Q}_{C_3H_8} = 0.044\ \text{kg s}^{-1}$, $T_s = 350\ \text{K}$
Outlet	Supersonic outlet	Supersonic outlet	–
Nozzle's walls	Slip adiabatic	Slip adiabatic	–
Other walls	No-slip adiabatic	No-slip adiabatic	–

Table 2
Summary of the numerical method used.

Type	CEDRE	AVBP
Spatial integration	MUSCL (2nd–3rd order)	TTGC – 3rd order
Time integration	Gear (2nd order implicit)	TTGC – 3rd order (explicit)
Combustion model	TPaSR	TFLES
Time Step	4×10^{-6}	2.6×10^{-7}

Finally, numerical parameters for each simulation are summarized in Table 2. The subgrid model for turbulence is the classical Smagorinsky closure [14,15] for both codes. Different combustion models are used and are described in the following section.

4.2. Combustion model: AVBP

To handle flame/turbulence interactions in AVBP [16], the Dynamically Thickened Flame model (DTFLES) is used [17]. This model thickens the flame front by a factor F so that it is resolved on the LES grid. To properly reproduce the effect of the subgrid scale interaction between turbulence and chemistry, the so-called efficiency function, E [18] is introduced to recover the turbulent flame speed. The DTFLES model has been applied successfully to several configurations (premixed and partially premixed) and more details can be found in [19].

The AVBP simulation uses a global one-step irreversible chemical scheme taking into account five species: $C_3H_8 + 5O_2 \rightarrow 3CO_2 + 4H_2O$. The reaction rate for this reaction reads:

$$q = f(\phi) \times A \times \left(\frac{\rho Y_{C_3H_8}}{W_{C_3H_8}}\right)^{0.856} \times \left(\frac{\rho Y_{O_2}}{W_{O_2}}\right)^{0.503} \times \exp\left(-\frac{E_a}{RT}\right) \tag{1}$$

with a pre-exponential factor $A = 3.2916 \times 10^{10}$ [cgs] and an activation energy $E_a = 31.126\ \text{cal mol}^{-1}$. $f(\phi)$ allows one to correctly predict laminar flame speed for an extended range of equivalence ratio. It reads:

$$f(\phi) = \frac{1}{2}\left[1 + \tanh\left(\frac{0.8 - \phi}{1.5}\right)\right] + \frac{2.11}{4}\left[1 + \tanh\left(\frac{\phi - 0.11}{0.2}\right)\right]\left[1 + \tanh\left(\frac{1.355 - \phi}{0.24}\right)\right] \tag{2}$$

Fig. 2 shows the comparison between detailed chemistry given by Peters [20] and this simplified one-step scheme for a given range of equivalent ratio. Laminar flame speed is well predicted whereas the adiabatic flame temperature is over-estimated with an error of around 7% at $\phi = 1$.

4.3. Combustion model: CEDRE

In the Transported Partially Stirred Reactor approach (TPaSR), one assumes that there is no flame front left (high Damköhler). At subgrid scale, pockets of reactants are mixed with a characteristic time linked to turbulence before they burn. This model has been used by Murrone and Scherrer [22] on a backward facing step combustion chamber and is built on two steps:

- First, a mixing step between reactants based on Eddy Dissipation Concept (EDC) model is devised as $C_3H_8 + O_2 \rightarrow C_3H_8^* + O_2^*$ where the "mixed" species denoted by * own the same thermodynamic properties as their initial

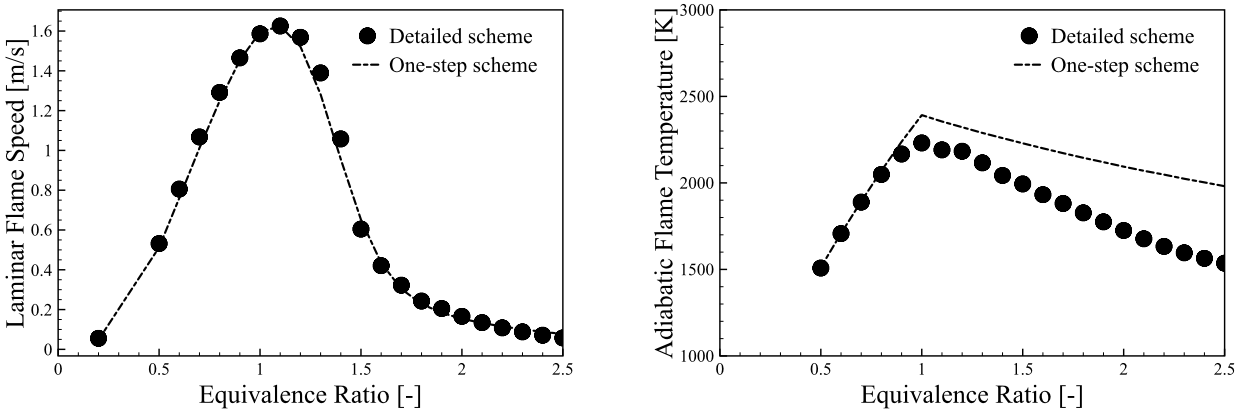

Fig. 2. Laminar flame speed (left) and adiabatic flame temperature (right) for the reference and simplified chemistry scheme (AVBP) and as functions of the equivalence ratio.

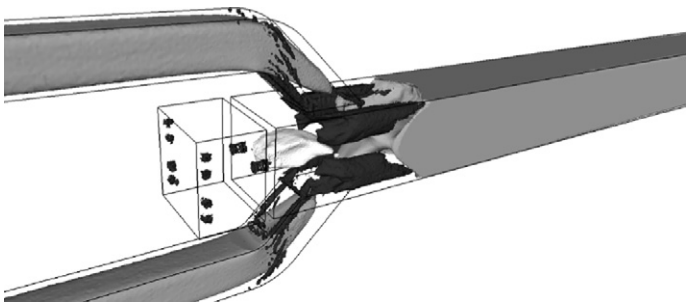

Fig. 3. Visualization of the main mean flow structures: "dome" recirculation zone ($u = -0.1U_{\text{bulk}}$) white iso-surface, axial velocity so-surface at U_{bulk} in gray and Q-criterion iso-surface in black. AVBP results. U_{bulk} stands for the bulk velocity in the air intake.

"un-activated" counter parts. This first step corresponds to a reaction that does not produce any heat release. The rate of progress of this equation reads $q = \min(Y_{C_3H_8}, Y_{O_2})/\tau_t$ where the frequency τ_t^{-1} is built on the LES filter width and the subgrid viscosity with $\tau_t^{-1} = (C_s T_{ij}^2)^{1/2}$ where T_{ij} is the deviatoric part of the resolved strain rate tensor and C_s a constant.

- Second, a kinetic step involving the "activated" reactants. In this study, a two-step reaction including CO dissociation is used [21]:

$$C_3H_8^* + 3.5O_2^* \longrightarrow 3CO + 4H_2O$$
$$CO + 0.5O_2^* \longleftrightarrow CO_2$$

5. Results

5.1. Mean flow topology

Fig. 3 depicts the main average structures of the flow inside the combustion chamber as obtained with AVBP. The impingement of the two jets defines two different zones: the "dome zone" in the head-end of the combustor where stands a strong recirculation zone and the zone upstream of the air intake. The two crushing jets coalesce into a velocity sheet inside the main ramjet duct. Note also that the two high speed jets are deflected at impact toward the walls creating four corner vortices through which fuel flows from the head-end to the downstream duct.

Fig. 4 shows the axial and vertical components of the velocity in the symmetry plane of the combustor (see Fig. 5a) and compared to experimental data. Flow predictions and measurements within the head-end are similar except for the reattachment point of the two jets. Indeed, quantities of interest differ in the air intakes: the bulk velocity is different. Separation where the air intakes curve appears to have a stronger effect in the AVBP simulation. Finally, flow topology

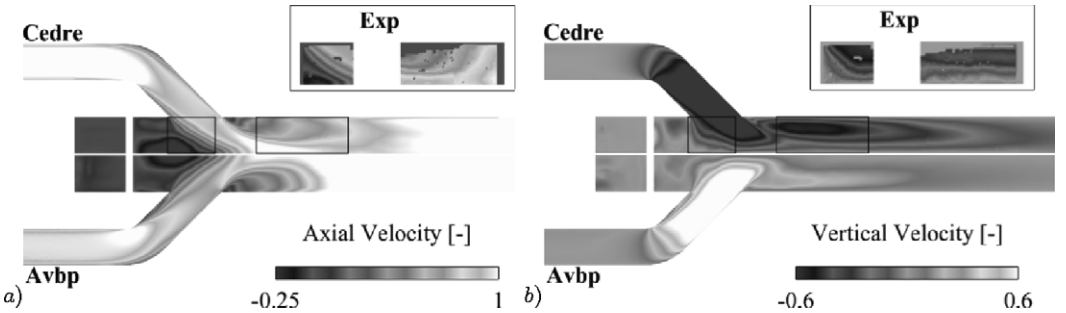

Fig. 4. Comparison of axial (a) and vertical (b) component of the velocity vector.

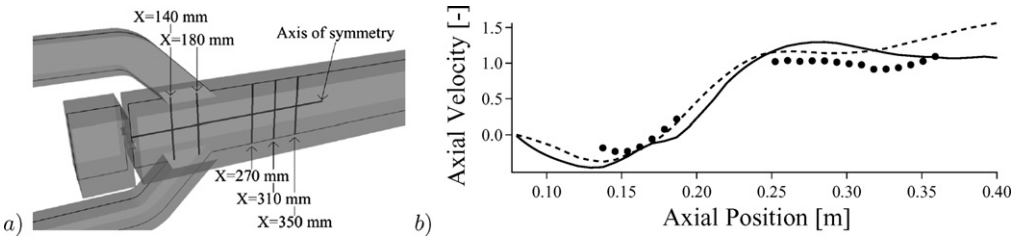

Fig. 5. Position of the profiles (a) and axial velocity evolution along the symmetry axis (b). •: Experiment; – –: AVBP; —: CEDRE. Values are non-dimensionalized by the bulk velocity in the air intake.

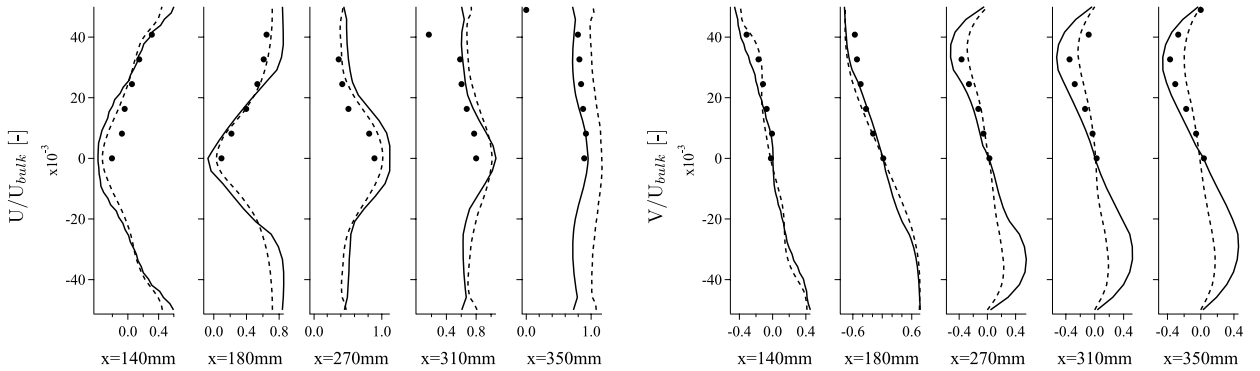

Fig. 6. Axial (left) and vertical (right) component of velocity vector along the y-axis (length in m). •: Experiment; – –: AVBP; —: CEDRE. Values are non-dimensionalized by the bulk velocity U_{bulk} in the air intake.

upstream the "dome zone" differs in the two simulations. AVBP predicts a quick opening of the coalesced jet sheet as shown by the experiment when CEDRE shows a more moderate acceleration of the flow in this region.

This behavior is emphasized in Fig. 5 where the evolution of the axial velocity along the symmetry axis of the ramjet is shown. Note that the magnitude of the velocity vector in the head-end of the chamber is over-estimated by both codes. As for the upper part of the combustor, AVBP reproduces the shape of the evolution of the axial velocity contrarily to CEDRE.

Fig. 6 shows profiles of axial and vertical components of the velocity along the y-axis as shown in Fig. 5. The AVBP simulation shows better results in the head-end of the chamber than far upstream the jet-on-jet impingement because of the wrong adiabatic flame temperature provided by the chemical scheme whereas CEDRE simulation yields good estimates of the axial velocity in this area. The vertical component of velocity differs only when the jet sheet opens upstream the air inlet. Taken as a whole, comparison against the experiment shows that the two LES codes yield good results in decent agreement with measurements at least for the mean quantities.

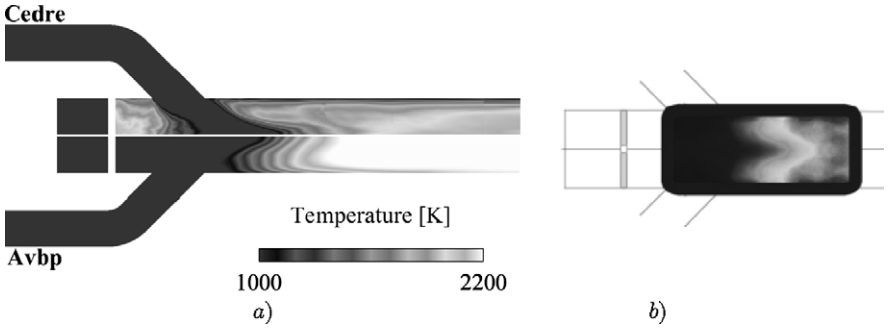

Fig. 7. Comparison of (a) the mean temperature field in the $z = 0$ mm plane and (b) the mean reacting zone from the experiment.

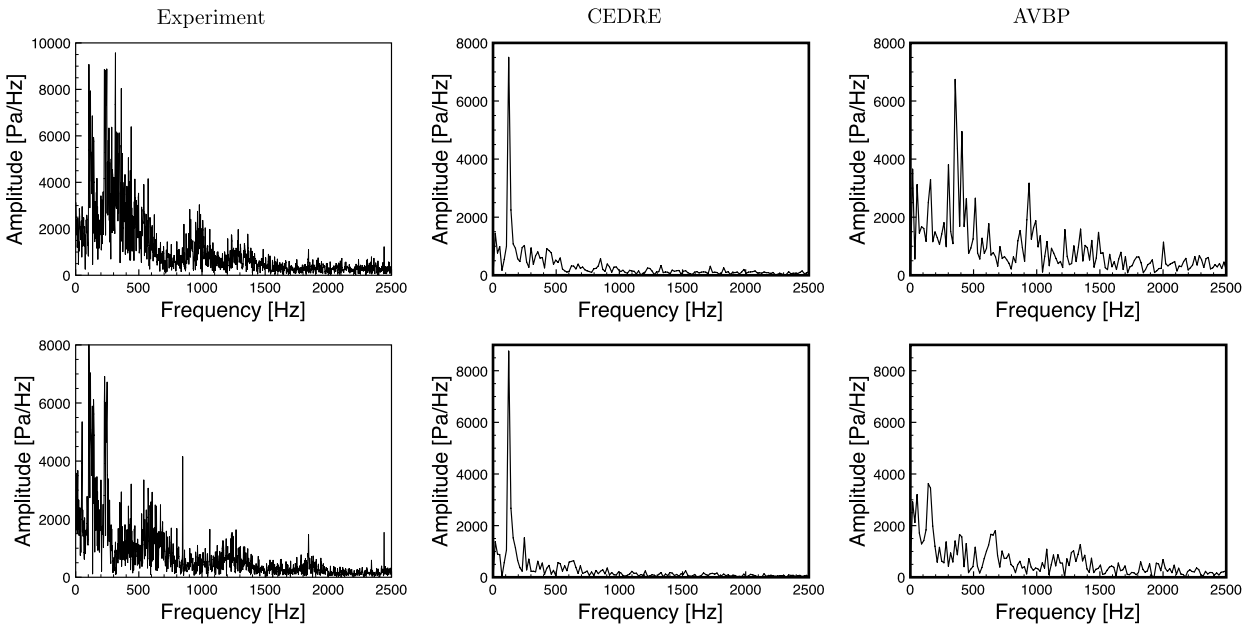

Fig. 8. Fourier transform of the pressure signal 100 mm (top) and 300 mm (bottom) upstream the air inlet.

Fig. 7 shows the mean temperature field as obtained with the two codes. The main dissemblance comes from the head-end of the combustor where reacting zones are identified in the CEDRE simulation and not in the AVBP one. The AVBP result is in concordance with experimental PLIF data that do not show OH emission in this zone.

5.2. Instantaneous results

To begin the analysis of the unsteady motion in the ramjet, Fourier Transforms (FT) of the pressure signal (obtained for a probe placed 100 mm and 300 mm upstream of the two air inlets) are displayed in Fig. 8. The duration of the signal for the two simulations is 56 ms yielding a frequency resolution of 18 Hz. Different peaks are visible in the experiment (see Table 3): around 120 Hz (Mode 1); 240 Hz (Mode 2) identified as a harmonic of the first frequency; a larger one between 300 and 360 Hz (Mode 3) and the last one at 950 Hz (Mode 4). CEDRE predictions exhibit one dominating frequency near Mode 1. Signals coming from the AVBP simulation is more disturbed and shows oscillations near the frequencies found experimentally.

The difference between the two simulations can be explained by the different shape of the temperature distribution inside the combustor. Fig. 9 shows spectral maps of the pressure signal extracted from the simulation using AVBP. For such maps, all the points of the configuration are treated based on LES snapshots. The associated frequency resolution

Table 3
Main frequencies detected in the LES simulations compared to the experimental data.

Mode	Frequency	Exp.	CEDRE	AVBP
1	120 Hz	Yes	Yes	Yes
2	240 Hz	Yes	Yes	Yes
3	300–360 Hz	Yes	No	Yes
4	950 Hz	Yes	No	Yes

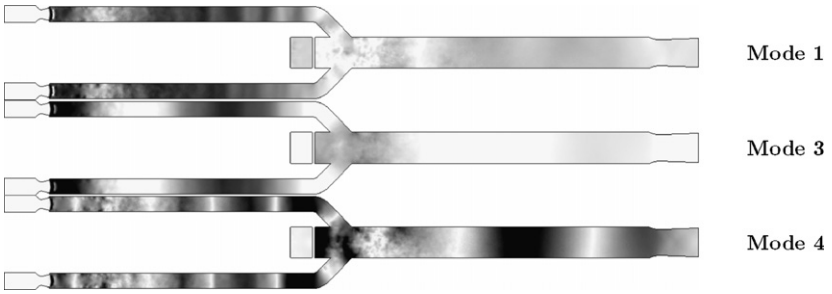

Fig. 9. Spectral maps of the pressure signal extracted for each point of the configuration: $|A_{\mathrm{FT}}^{\mathrm{freq}}(\mathbf{x}) \times \cos(\Phi_{\mathrm{FT}}^{\mathrm{freq}}(\mathbf{x}))|$ (AVBP results).

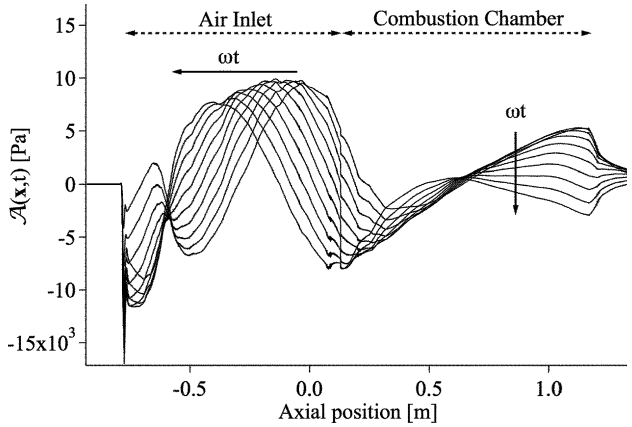

Fig. 10. Spatial and temporal evolution of the fluctuations of pressure at the frequency of **Mode 3**.

is 11 Hz. **Mode 3** appears to be a longitudinal acoustic mode. Fig. 10 displays the spatial evolution of the Fourier transform (FT) of the pressure signals for ten different times defined by:

$$\mathcal{A}(\mathbf{x}, t) = A_{\mathrm{FT}}^{\mathrm{freq}}(\mathbf{x}) \times \cos\left(\Phi_{\mathrm{FT}}^{\mathrm{freq}}(\mathbf{x}) + \omega_{\textbf{Mode 3}} \times t\right) \tag{3}$$

where $A_{\mathrm{FT}}^{\mathrm{freq}}(\mathbf{x})$ and $\Phi_{\mathrm{FT}}^{\mathrm{freq}}(\mathbf{x})$ are respectively the amplitude and the phase of the FTs. It shows that **Mode 3** is a $1/2$ wave acoustic mode of the main combustion chamber while pressure fluctuations in the air inlets are linked with the propagation of the acoustic waves coming from the head-end of the combustor toward the inlet's nozzles. **Mode 4** seems also to have an acoustic nature and concerns the whole geometry. **Mode 1** is different from the two latter and its nature is for the moment unclear.

The main frequency (Mode 3) appearing in the simulation using AVBP leads to a flow blockage (velocity nodes or pressure anti-nodes) in the end of the air inlet and the dome zone. Pressure fluctuations modulate the mass flow rate inside the head-end of the combustor as depicted by Fig. 11. Two snapshots, displayed on Fig. 12, taken within half a period of Mode 3 stress the impact of the pressure oscillation on combustion. The flow blockage has for primary effect to influence the impingement of the two air jets as well as the modulation of the four corner vortices. The fuel alimentation of the upstream dome zone is thus strongly influenced. The left picture emphasizes this phenomenon when the flow blockage disappears: part of the flame is anchored at the interface between the latter coherent structures

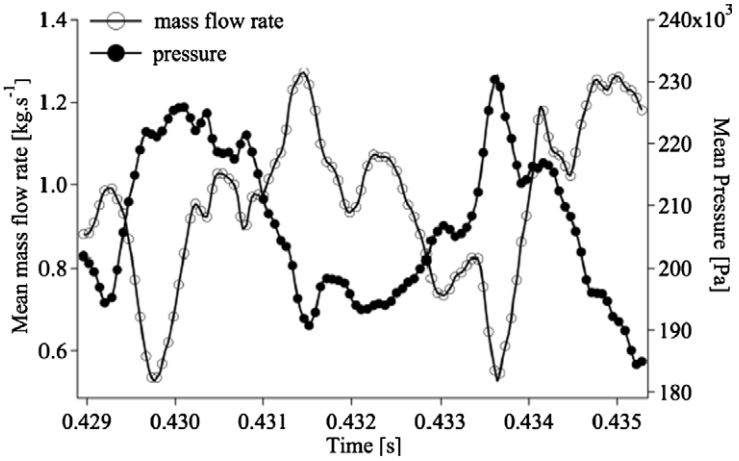

Fig. 11. Evolution of mass flow rate and pressure in a plane in the main chamber at the exit of the air inlets. Two periods of Mode 3 are displayed.

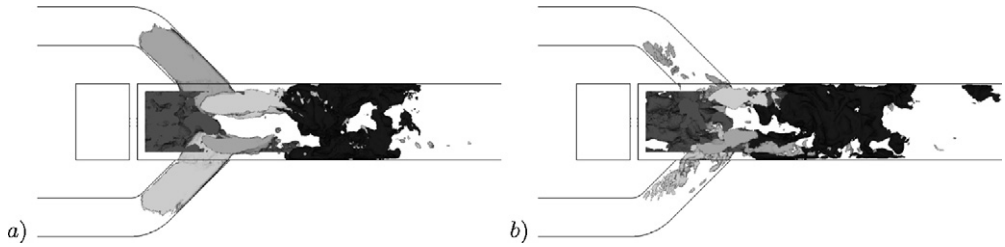

Fig. 12. Instantaneous fields: iso-volume of non-dimensionalized vertical component of velocity (0.9 in white and -0.9 in light gray), iso-volume of zero axial component of velocity in dark gray and iso-volume of reaction rate at 10^3 J mol^{-1} s^{-1} in dark. These views are taken within half a period of Mode 3.

and the recirculation zone created by the flow blockage. When the velocity is maximum, the dome is free from fresh air. Strong recirculations are created in this area but as the equivalent ratio is too high, combustion is damped. When the flow blockage appears, recirculation zones are released upstream, both in the central part of the combustion chamber and along the corner vortices feeding the flame with fuel. Different combustion regimes are identified. First, as packets of fuel are released upstream, they ignite thanks to diffusion flames at the outskirt part. The topology of the flame along the vortices is different: triple flames are identified allowing a higher turbulent flame velocity.

Flames in the "Research Ramjet" are thus stabilized mainly by the corner vortices. However, modulation of mass flow rate gives a horizontal movement to the flame which is compensated by the packets released at the end of the flow blockage.

6. Conclusion

Two LES were performed to simulate the reacting flow field in a ramjet-like combustor. Although the two codes are very different numerically, both predictions are in good agreement with the experiment for the mean velocity field. First differences between the two predictions come from the chemistry and combustion models. Dynamically Thickened Flame for Large Eddy Simulation model and a chemistry able to simulate the evolution of laminar flame speed for an extended range of equivalent ratios show good agreement with experimental data for the mean reacting zone and the evolution of the axial velocity within the dump combustor. The TPaSR approach model with chemical scheme of Westbrook & Dryer allowing combustion for high equivalent ratio predicts reacting zones in the head-end of the chamber. These differences strongly impact the energy contained motions of both simulations. For CEDRE, only one frequency arises while four modes coexist with AVBP. Detailed analyses of AVBP predictions point to acoustics as a driving mechanism in determining the stability of the burner. Absence of the two identified acoustic modes in the simulation using CEDRE could be explained by different points:

- The computation has been handled using implicit time advancement with acoustic CFL number higher than one inducing increased dispersion and dissipation throughout the frequency range. Local effects can thus be miss-represented although they participate to the amplification of low frequency phenomena as found in the experiment.
- One crucial mechanism in the expression of all the frequency peaks observed in the experiment is the temperature field issued by the hot gazes in the head-end. This oscillation modifies the sound speed in this zone and impacts directly the acoustic mode potentially present in the ramjet.

Further work will consist in isolating the different points that can affect the predictions: currently, a simulation using CEDRE with TFLES model and the same chemistry as in AVBP will allow to look at the effects of time advancement. The impact of chemistry is also investigated by comparing two different simulations with AVBP where the correction of the pre-exponential is activated or not.

Acknowledgements

The simulation with AVBP used resources of the Argonne Leadership Computing Facility at Argonne National Laboratory, supported by the Office of Science of the U.S. Department of Energy under contract DE-AC02-06CH11357. Supports of the French Délégation générale pour l'armement (DGA) and also of M. Alain Cochet, head of the "Airbreathing Propulsion research unit" from the Fundamental and Applied Energetics Department of Onera are gratefully acknowledged.

References

[1] T. Poinsot, D. Veynante, Theoretical and Numerical Combustion, 2nd edition, R.T. Edwards, 2005.
[2] H. Pitsch, Large eddy simulation of turbulent combustion, Ann. Rev. Fluid Mech. 38 (2006) 453–482.
[3] P. Sagaut, Large Eddy Simulation for Incompressible Flows, Scientific Computation Series, Springer-Verlag, 2000.
[4] M. Boileau, G. Staffelbach, B. Cuenot, T. Poinsot, C. Bérat, LES of an ignition sequence in a gas turbine engine, Combust. Flame 154 (1–2) (2008) 2–22.
[5] B. Sjöblom, Full-scale liquid fuel ramjet combustor tests, in: IXth ISABE, vol. 7027, 1989, pp. 273–281.
[6] J.-M. Samaniego, B. Yip, T. Poinsot, S. Candel, Low-frequency combustion instability mechanism in a side-dump combustor, Combust. Flame 94 (4) (1993) 363–381.
[7] D.E. Rogers, F.E. Marble, A mechanism for high frequency oscillations in ramjet combustors and afterburners, Jet Propul. 26 (1956) 456–462.
[8] L.Y.M. Gicquel, Y. Sommerer, B. Cuenot, T. Poinsot, LES and acoustic analysis of turbulent reacting flows: Application to a 3D oscillatory ramjet combustor, in: ASME, Paper AIAA-2006-151, RENO, USA, 2006.
[9] S. Reichstadt, N. Bertier, A. Ristori, P. Bruel, Towards LES of mixing processes inside a research ramjet combustor, in: ISABE, 2007, p. 1188.
[10] A. Roux, L.Y.M. Gicquel, Y. Sommerer, T. Poinsot, Large eddy simulation of mean and oscillating flow in side-dump ramjet combustor, Combust. Flame 152 (1–2) (2008) 154–176.
[11] G. Heid, A. Ristori, Local fuel concentration measurements in a research dual ramjet combustion chamber by gas sampling analysis with carbon dioxide injection at the head end of the combustor, in: XVIIth Symposium ISABE, Munich, Germany, 2005.
[12] A. Ristori, G. Heid, A. Cochet, G. Lavergne, Experimental and numerical study of turbulent flow inside a dual inlet research ducted rocket combustor, in: XIVth Symposium ISABE, Florence, Italy, 1999.
[13] A. Ristori, G. Heid, C. Brossard, S. Reichstadt, Detailed characterization of the reacting one-phase and two-phase flow inside a research ramjet combustor, in: XVIIth Symposium ISABE, Munich, Germany, 2005.
[14] J. Smagorinsky, General circulation experiments with the primitive equations. i. The basic experiment, Mon. Weather Rev. 91 (3) (1963) 99–165.
[15] M. Germano, Turbulence: the filtering approach, J. Fluid Mech. 238 (1992) 325–336.
[16] N. Lamarque, Schémas numériques et conditions limites pour la simulation aux grandes échelles de la combustion diphasique dans les foyers d'hélicoptères, Ph.D. thesis, INP Toulouse, 2007.
[17] J.-Ph. Légier, T. Poinsot, D. Veynante, Dynamically thickened flame large eddy simulation model for premixed and non-premixed turbulent combustion, in: Summer Program 2000, Center for Turbulence Research, Stanford, USA, 2000, pp. 157–168.
[18] O. Colin, F. Ducros, D. Veynante, T. Poinsot, A thickened flame model for large eddy simulations of turbulent premixed combustion, Phys. Fluids 12 (7) (2000) 1843–1863.
[19] P. Schmitt, T.J. Poinsot, B. Schuermans, K. Geigle, Large-eddy simulation and experimental study of heat transfer, nitric oxide emissions and combustion instability in a swirled turbulent high pressure burner, J. Fluid Mech. 570 (2007) 17–46.
[20] N. Peters, B. Rogg, Reduced Kinetic Mechanisms for Applications in Combustion Systems, Lecture Notes in Physics, Springer-Verlag, Heidelberg, 1993.
[21] C. Westbrook, F. Dryer, Simplified reaction mechanism for the oxidation of hydrocarbon fuels in flames, Combust. Sci. Technol. 27 (1981) 31–43.
[22] A. Murrone, D. Scherrer, Large-eddy simulation of a turbulent premixed flame stabilized by a backward facing step, in: 1st INCA Workshop, Villaroche, France, 2005.